

Expanded atlas of the sky in continuous gravitational waves

Vladimir Dergachev^{1, a} and Maria Alessandra Papa^{1, 2, b}

¹Max Planck Institute for Gravitational Physics (Albert Einstein Institute), Callinstraße 38, 30167 Hannover, Germany

²Leibniz Universität Hannover, D-30167 Hannover, Germany

We present the full release of the atlas of continuous gravitational waves, covering frequencies from 20 Hz to 1700 Hz and spindowns from -5×10^{-10} to 5×10^{-10} Hz/s. Compared to the early atlas release, we have extended the frequency range and have performed follow-up on the outliers. Conducting continuous wave searches is computationally intensive and time-consuming. The atlas facilitates the execution of new searches with relatively minimal computing resources.

I. INTRODUCTION

Continuous gravitational waves are very weak nearly monochromatic signals that are much harder to detect than coalescences of binary black holes or neutron stars.

One expects continuous waves from rapidly rotating neutron stars, if they present a sustained non-axisymmetric deformation ε . The intrinsic amplitude of the gravitational wave signal is proportional to the deformation, increases with the square of the signal frequency f and decreases with the inverse of the distance to the source d :

$$h_0 = \frac{4\pi^2 G I_{zz} f_0^2 \varepsilon}{c^4 d}, \quad (1)$$

with $I_{zz} = 10^{38}$ kg m² being the moment of inertia of the star with respect to the principal axis aligned with the rotation axis.

Gravitational waves carry away energy, which slows pulsar rotation. Observations of pulsars provide data on the spin and spin-down rates of neutron stars and suggest that their deformations are very small. This is also supported by the non-detections of increasingly sensitive surveys [1–4] and population studies [5]. We hence have developed the Falcon search that excels at searches for small-deformation objects [6–9].

Since all-sky searches for continuous gravitational waves like ours are very computationally intensive, we have started releasing large-scale data from our Falcon surveys for others to use in their own analyses, e.g. to follow-up, to cross-correlate with other astrophysical probes or for coincidences with their own gravitational wave search results on other data sets. We call such releases “the atlas” [10], as they comprehensively cover the sky in many searched frequency bands.

Our last release [11] was from an all-sky search on LIGO O3a data [1] for signals with frequency up to 1500 Hz. We shared that atlas even before completing the follow-up of the most interesting results. Here we report results of the full follow-up, including a cross-check against the O3b data [12]. 509 outliers pass our follow-up pipeline using O3a data, and of those only 22 survives

the cross-check against O3b data. Of those 22 outliers, one is attributed to a detector artefact, while the rest are due to simulated signals injected during the O3 science run.

The results presented here cover signal frequencies up to 1700 Hz, which represents a 50% increase in the searched parameter space volume with respect to [11], as the number of templates increases with the cube of the frequency.

A new release of the atlas is associated with these results. The atlas includes SNR data and upper limits on

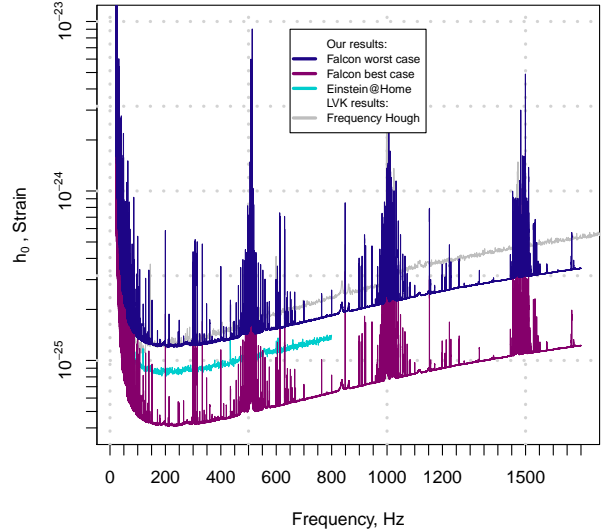


FIG. 1. Gravitational wave intrinsic amplitude h_0 upper limits at 95% confidence as a function of signal frequency. The upper limits measure the sensitivity of the search. We also plot latest LIGO/Virgo and Einstein@Home all-sky population average results [2, 4, 11].

the intrinsic gravitational wave amplitude h_0 as a function of sky position and frequency. The upper limits are provided for worst-case wave polarization and best-case (circular) polarization. Arbitrary polarization upper limits can be computed for the inclination angle ι and polarization angle ψ of interest using Eq.s (20) and (21) in [13] with the parameter values c_{1-14} provided in the

^a vladimir.dergachev@aei.mpg.de

^b maria.alessandra.papa@aei.mpg.de

atlas. The upper limits have been established across the entire frequency band with no exclusions. The upper limits maximized over sky-position are shown in Figure 1.

II. THE SEARCH

Stage	Coherence length (days)	Minimum SNR
1	0.5	6
2	1	8
3	2	9
4	6	16

TABLE I. Parameters for each stage of the search. Stage 4 refines outlier parameters by using denser sampling of the parameter space and then subjects them to an additional consistency check by comparing outlier parameters from analyses of individual interferometer data. Only the first two stages were used to construct the atlas, while subsequent stages were used for outlier analysis.

Our search used O3a data for the main analysis, with crosscheck performed against O3b data. The setup was previously described in [11]. The extension to 1700 Hz was performed without any modifications. As before, the upper limits were derived using the universal statistics [14], which infers the absence of signals with amplitude above a certain level based on the level of power in the underlying data. The universal statistics is designed to be valid for data arbitrarily distributed and hence we do not need compute-intensive Monte Carlos to establish upper limits. We have carried some Monte Carlo campaigns testing the signal-recovery capabilities of our pipeline on fake signals for validation purposes.

The outlier follow-up is new to this paper and used 4 stages, as shown in Table I. Through stages 2-4 the coherence length increases and the size the region covered by a loosely coherent template decreases, and this results in refined outlier parameters. At every stage only candidates with SNR above a given threshold are passed to the next stage. The thresholds are chosen to be deliberately low to reduce the likelihood of losing detections due to overly aggressive SNR cutoff.

Each outlier from stage 4 is further checked for consistency across the different detector combinations, namely using O3a data in single- and multi-interferometer searches, again using the stage 4 setup. We require outlier parameters from these different searches to be consistent, and discard outliers with frequency mismatch $> 2 \mu\text{Hz}$ or with spindown mismatch $> 0.3 \text{pHz/s}$. The outliers that pass this check are included with this paper [15].

The crosscheck with O3b data was performed last, using a very simple requirement that the outlier frequency be within $10 \mu\text{Hz}$ between O3a and O3b datasets. The O3b searches also use the stage 4 setup. Our simulations

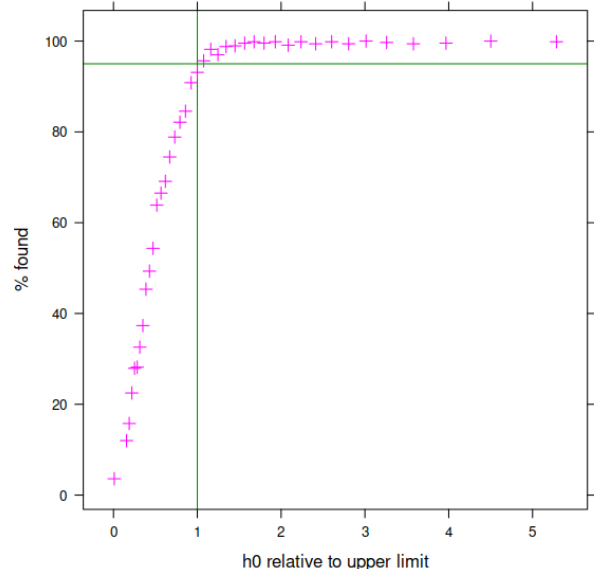


FIG. 2. Injection recovery versus injection strain normalized to the upper limit established on the same data without injection.

show that this results in recovery of 95% of injections with strength above upper limit value (Figure 2).

The full list of outliers that passed O3b cross-check is shown in Table II. All except one correspond to one of hardware-injected simulated signals (Table III).

The outlier at 20.5 Hz is associated with a known low-frequency comb of instrumental artifacts [16].

Out of eight hardware-injected signals within our parameter space, we detected 6. The two missed signals, ip10 and ip11, are located in a highly contaminated low-frequency region.

The injection ip10 has templates in both O3a and O3b data but is rejected by the coincidence check because the H1 interferometer lacks the sensitivity to detect it.

The injection ip11 is a factor of 4 below the upper limit and does not progress to the stage 4 follow-up.

III. CONCLUSIONS

We have performed a wide-band search of O3a data covering frequencies from 20 to 1700 Hz. No significant outliers have passed the cross-check with O3b data during follow-up. The high frequency extension allows us to expand the best-case reach of our search to 250 pc for $\epsilon > 10^{-8}$. We make the atlas of upper limits, signal-to-noise ratios and associated data available for further study.

SNR	f Hz	\dot{f} pHz/s	RA _{J2000} degrees	DEC _{J2000} degrees	iota degrees	psi degrees	$f_{O3a} - f_{O3b}$ μ Hz	$f_{O3a} - f_{inj}$ μ Hz	$\dot{f}_{O3a} - \dot{f}_{inj}$ pHz/s	dist _{inj} arcsec
55.6	20.50003	0.0	269.7440	66.5787	135.00	80.00	-8.2			
439.8	52.80832	0.2	302.6456	-83.8261	56.25	72.00	-5.3	-0.7	0.2	47.4
440.5	52.80832	-0.0	302.6316	-83.8374	56.25	72.00	3.4	-0.2	0.0	6.4
445.4	52.80832	0.0	302.6428	-83.8390	56.25	72.00	-0.5	-0.2	0.0	6.2
433.3	52.80832	-0.0	302.6646	-83.8368	56.25	72.00	-2.4	-0.2	0.0	17.0
435.7	52.80832	0.2	302.5930	-83.8244	56.25	72.00	-0.5	-0.2	0.2	54.7
436.0	52.80832	0.0	302.6642	-83.8378	56.25	72.00	0.5	-0.2	0.0	15.3
435.7	52.80832	0.2	302.5929	-83.8244	56.25	72.00	-0.5	-0.2	0.2	54.7
436.6	52.80832	-0.0	302.6570	-83.8370	56.25	72.00	0.5	-0.2	0.0	14.0
434.2	52.80832	-0.4	302.7008	-83.8673	56.25	72.00	5.8	0.3	-0.4	105.3
433.5	52.80832	-0.4	302.6881	-83.8642	56.25	72.00	5.8	0.3	-0.4	93.2
441.6	52.80832	-0.4	302.6930	-83.8651	56.25	72.00	5.8	0.3	-0.4	96.7
55.4	108.85716	0.0	178.3665	-33.4376	101.25	30.00	0.5	-0.3	0.0	18.6
55.4	108.85716	-0.0	178.3750	-33.4342	101.25	30.00	-3.4	0.1	0.0	11.5
82.4	265.57505	-4.4	71.5535	-56.2150	45.00	50.00	4.3	0.0	-0.2	9.5
82.2	265.57505	-4.0	71.5510	-56.2180	45.00	50.00	-2.4	0.0	0.2	2.7
84.9	265.57505	-4.0	71.5512	-56.2180	45.00	50.00	-2.4	0.0	0.2	2.5
85.3	265.57505	-3.8	71.5509	-56.2220	45.00	50.00	-5.8	0.5	0.3	16.2
100.1	575.16350	-0.4	215.2574	3.4481	135.00	60.00	6.3	-1.2	-0.3	15.6
98.7	575.16351	0.2	215.2575	3.4416	135.00	70.00	-6.8	-0.3	0.3	9.7
110.7	763.84732	0.4	198.8926	75.6906	123.75	9.00	-1.4	-1.2	0.4	7.3
1055.5	848.93498	-300.0	37.3940	-29.4525	67.50	22.50	0.5	0.1	0.0	0.6

TABLE II. Outliers produced by the detection pipeline that passed the coincidence check with O3b data. All outliers except the one at 20.5 Hz are due to simulated signals “hardware-injected” during the science run for validation purposes. Their parameters are listed in Table III. The last three columns show differences between outliers and injection frequency, frequency derivative, and location on the sky. Signal frequencies refer to GPS epoch 1246070000 (2019 Jul 2 02:33:02 UTC).

-
- [1] The O3a Data Release <https://doi.org/10.7935/nfnt-hm34>
- [2] B. Steltner, M. A. Papa, H. B. Eggenstein, R. Prix, M. Bensch, B. Allen and B. Machenschalk, Deep Einstein@Home All-sky Search for Continuous Gravitational Waves in LIGO O3 Public Data, *Astrophys. J.* **952**, no.1, 55 (2023)
- [3] R. Abbott *et al.* (LIGO Scientific Collaboration, Virgo Collaboration and KAGRA Collaboration), All-sky search for continuous gravitational waves from isolated neutron stars in the early O3 LIGO data, *Phys. Rev. D* **104**, 082004 (2021)
- [4] R. Abbott *et al.* (LIGO Scientific Collaboration, Virgo Collaboration and KAGRA Collaboration), All-sky search for continuous gravitational waves from isolated neutron stars using Advanced LIGO and Advanced Virgo O3 data, *Phys. Rev. D* **106**, 102008 (2022)
- [5] G. Pagliaro, M. A. Papa, J. Ming, J. Lian, D. Tsuna, C. Maraston and D. Thomas, Continuous Gravitational Waves from Galactic Neutron Stars: Demography, Detectability, and Prospects, *Astrophys. J.* **952**, no.2, 123 (2023)
- [6] V. Dergachev, On blind searches for noise dominated signals: a loosely coherent approach, *Class. Quantum Grav.* **27**, 205017 (2010).
- [7] V. Dergachev, Loosely coherent searches for sets of well-modeled signals, *Phys. Rev. D* **85**, 062003 (2012)
- [8] V. Dergachev, Loosely coherent searches for medium scale coherence lengths, arXiv:1807.02351
- [9] Sensitivity Improvements in the Search for Periodic Gravitational Waves Using O1 LIGO Data Sensitivity Improvements in the Search for Periodic Gravitational Waves Using O1 LIGO Data, V. Dergachev and M. A. Papa, *Phys. Rev. Lett.* **123**, no. 10, 101101 (2019)
- [10] Vladimir Dergachev and Maria Alessandra Papa, Frequency-Resolved Atlas of the Sky in Continuous Gravitational Waves, *Phys. Rev. X* **13**, 021020 (2023)
- [11] Vladimir Dergachev and Maria Alessandra Papa, Early release of the expanded atlas of the sky in continuous gravitational waves, *Phys. Rev. D* **109**, 022007 (2024) doi:10.1103/PhysRevD.109.022007
- [12] The O3b Data Release <https://doi.org/10.7935/pr1e-j706>
- [13] Vladimir Dergachev, Efficient representations of upper limits and confidence intervals for experimental data, *Phys. Rev. D* **110**, 085001 (2024)
- [14] V. Dergachev, A Novel Universal Statistic for Computing Upper Limits in Ill-behaved Background, *Phys. Rev. D* **87**, 062001 (2013).
- [15] See EPAPS Document No. [number will be inserted by publisher] for numerical values of upper limits. Also at <https://www.atlas.aei.uni-hannover.de/work/volodya/releases.html> including the full atlas.
- [16] <https://gwosc.org/O3/o3speclines/>

Label	f Hz	\dot{f} Hz/s	SNR	UL/ h_0 %	Δf mHz	In	Found
ip0	265.57505	-4.15e-12	28.5	122.5	-0.1	Yes	Yes
ip1	848.93498	-3e-10	393.0	119.9	-0.1	Yes	Yes
ip2	575.16351	-1.37e-13	39.3	138.5	0.0	Yes	Yes
ip3	108.85716	-1.46e-17	23.7	141.6	0.1	Yes	Yes
ip4	1390.60583	-2.54e-08	7.6	21.3	-7.7	No	No
ip5	52.80832	-4.03e-18	155.9	130.2	0.0	Yes	Yes
ip6	145.39178	-6.73e-09	8.4	25.0	-11.2	No	No
ip7	1220.42586	-1.12e-09	7.3	68.1	3.6	No	No
ip8	190.03185	-8.65e-09	8.9	83.8	-2.9	No	No
ip9	763.84732	-1.45e-17	39.1	135.1	0.1	Yes	Yes
ip10	26.33210	-8.5e-11	63.9	124.9	0.0	Yes	No
ip11	31.42470	-5.07e-13	93.2	400.9	-12.1	Yes	No
ip12	37.75581	-6.25e-09	14.0	156.5	4.0	No	No
ip16*	234.56700	0	8.3	29.6	42.7	No	No
ip17*	890.12300	0	8.1	103.6	23.6	No	No

TABLE III. This table shows parameters of the hardware-injected continuous wave signals and atlas data for their locations and frequencies. The signals ip16 and ip17 have binary modulation applied. The upper limits for the injections are polarization-specific and were computed using ι and ψ of each injection. We show all the hardware injections within 20-1700 Hz range, including those outside of our search space, as indicated by the “In” column. We use the reference time (GPS epoch) $t_0 = 1246070000$ (2019 Jul 2 02:33:02 UTC).